

Size distribution and elemental compositions of anhydrous minerals in the Ryugu samples C0224 and C0260: Implications for radial transport mechanism and source regions of anhydrous minerals

D. Nakashima¹, M. Matsumoto¹, H. Yoshida², T. Mikouchi², T. Nakamura¹

¹Tohoku University, Japan (dnaka@tohoku.ac.jp), ²University of Tokyo, Japan.

Introduction: Samples returned from C-type asteroid Ryugu by the Hayabusa2 spacecraft are mineralogically and chemically similar to CI chondrites [1-4]. It was suggested from the initial analysis of the Ryugu samples that the Ryugu original parent body formed beyond the H₂O and CO₂ snow lines (> 3 – 4 au) in the solar nebula at 1.8 – 2.9 Myr after CAI formation [1]. Nakashima et al. [5] reported elemental compositions and oxygen isotope ratios of chondrule-like objects and Ca-Al-rich inclusions (CAIs) in the Ryugu samples. The objects (< 30 μm) are as small as those from comet Wild2, suggesting radial transport favoring smaller objects from the inner solar nebula (solar neighborhood and chondrule formation regions) to the formation location of the Ryugu original parent body, which is farther from the Sun and scarce in chondrules [5]. Besides chondrule-like objects and CAIs, anhydrous minerals such as olivine, pyroxene, spinel, and hibonite occur in the Ryugu samples and are much more abundant [1]. In the present study, we measured size distribution of anhydrous minerals in the newly allocated Ryugu samples (C0224 and C0260) using FE-SEM and FE-EPMA to test the hypothesis of radial transport favoring smaller objects [5] and elemental compositions to elucidate the source regions of individual anhydrous minerals.

Results: Synchrotron radiation X-ray computed tomography at SPring-8 showed that C0224 has a homogeneous lithology except for the presence of large carbonate crystals of few hundred μm in size and C0260 contains clasts with different lithologies. Three hundred ten anhydrous minerals including chondrule-like objects were found in eight polished sections from C0260 (C0260-01, 02, and 03) and C0224 (C0224-01, 02, 03, 04, and 05), and most of them were from C0260. Polished sections of C0224 were repolished multiple times but only 6 grains were observed. Most anhydrous minerals occur along with calcite, Ca phosphate, and Na-Mg phosphate in FeO-rich phyllosilicate regions, which is characteristic for lithology II clasts (less-altered clasts; [6]). Anhydrous minerals have angular shapes, so that diameters are calculated from surface areas of anhydrous minerals using ImageJ assuming they have spherical shapes. The largest one is 24 μm and smallest one is 0.5 μm. As shown in [Fig. 1a](#), the peak of size distribution of anhydrous minerals including chondrule-like objects occurs at 2 – 3 μm. It should be noted that we counted anhydrous minerals detected by FE-SEM mapping, and therefore there is counting loss of tiny minerals (<< 1 μm). Olivine is most abundant followed by spinel, pyroxene, and hibonite. Mg#’s of olivine are from 89.5 to 99.4, which is consistent with the initial analysis [1]. Low-iron manganese-enriched (LIME) olivine with MnO/FeO ratio (wt%) exceeding 1 [7] is observed. Pyroxene and hibonite grains are too small to obtain precise compositions. Spinel contains variable amounts of Cr₂O₃ (0.21 – 4.0 wt%).

Six chondrule-like objects are observed ([Fig. 1b](#)). They have rounded shapes and mainly consist of FeO-poor olivine with Mg# from 92.0 to 99.2 along with diopside, rounded (oxidized) Fe-Ni metal, and altered phase. The chondrule-like objects are similar to those found in the initial analysis [1,5].

Discussion: Most anhydrous minerals occur in less-altered clasts in the Ryugu samples [1, this study]. The clasts have protected anhydrous minerals from aqueous alteration and brecciation for ~ 4.6 Gyr, so that sizes of the anhydrous minerals reflect those during accretion onto the Ryugu original parent body. Our new data ([Fig. 1a](#)) show that anhydrous minerals in the Ryugu samples (< 24 μm) are smaller than chondrules in chondrites (~ 500 μm; [8]) and isolated olivine in chondrites (> 20 μm; [9]), suggesting radial transport favoring smaller objects to the formation location of the Ryugu original parent body. There are two possible mechanisms for radial transport: a combination of advection and turbulent diffusion [10] and photophoresis [11]. Both mechanisms can transport grains smaller than 30 μm. While the Ryugu original parent body formed at ~ 2 Myr after the CAI formation [1], photophoresis transports 10 μm grains beyond 10 au later than ~ 5 Myr after the CAI formation [11]. Considering the time window, a combination of advection and turbulent diffusion that transports ≤ 20 μm grains beyond 25 au within 1 Myr [10] would be more likely for Ryugu. It will be more plausible by size distributions of anhydrous minerals in other Ryugu samples and CI chondrites.

Olivine in type I chondrules is more enriched in Cr₂O₃ and CaO than olivine in amoeboid olivine aggregates (AOAs) ([Fig. 2a](#)) [5]. ¹⁶O-rich chondrule-like objects, CAIs, and ¹⁶O-rich olivine in the Ryugu samples are distributed in the AOA area, while ¹⁶O-poor chondrule-like object and ¹⁶O-poor olivine are distributed in the type I chondrule area. The difference in the elemental compositions of olivine with different origins is explained by AOA olivine condensation from a residual gas depleted in the refractory elements followed by isolation from the gas before condensation of Cr [5]. Olivine depleted in Cr₂O₃ and CaO may have formed

near the Sun, and olivine relatively enriched in the two elements may have formed in the chondrule formation regions. Thus, it is possible to deduce the source regions of isolated olivine and chondrule-like objects based on the Cr_2O_3 and CaO concentrations. Many of isolated olivine grains and olivine in chondrule-like objects in C0260 and C0224 distribute in the AOA area (Fig. 2b), which is consistent with the FE-EPMA analysis of olivine in CI chondrites [12]. The AOA-like olivine may have formed near the Sun. It is considered from the high abundance of AOA-like olivine in the Ryugu samples and frequent occurrence of ^{16}O -rich olivine in Wild2 particles [13] that olivine formed near the Sun were transported to the outer regions of the early solar nebula and survived due to lack of chondrule forming event that erases ^{16}O -rich signature and original elemental compositions. On the contrary, isolated olivine in chondrites distributes in the type I chondrule area (Fig. 2c), and ^{16}O -rich olivine is rare in chondrites [14]. It is considered that ^{16}O -rich olivine passed the chondrule formation regions and/or melted during chondrule forming events.

Nakashima et al. [5] reported that spinel in the Ryugu CAIs contain small amounts of Cr_2O_3 with < 0.2 wt% and suggested that the CAIs escaped from remelting event and may be as old as the oldest CAIs. Isolated spinel in C0260 show variable Cr_2O_3 concentrations up to 4.0 wt%. Therefore, spinel that acquired Cr by remelting events are also present in the Ryugu samples. Considering the time window of accretion (within ~ 2 Myr after CAI formation; [1]), remelting events may have occurred during that period.

References: [1] Nakamura T. et al. (2022) *Science* 10.1126/science.abn8671. [2] Ito M. et al. (2022) *Nat. Astron.* 10.1038/s41550-022-01745-5. [3] Nakamura E. et al. (2022) *Proc. Jpn. Acad. Ser. B* 98:227. [4] Yokoyama T. et al. (2022) *Science* 10.1126/science.abn7850. [5] Nakashima D. et al. (2023) *Nat. Commun.* 14:532. [6] Mikouchi T. et al. (2022) LPSC LIII, #1935. [7] Klöck W. et al. (1989) *Nature* 339:126. [8] Friedrich J. M. et al. (2015) *Chem. Erde* 75:419. [9] Jacquet E. et al. (2021) *M&PS* 56:13. [10] Hughes A.L.H. & Armitage P.J. (2010) *ApJ* 719:1633. [11] Moudens A. et al. (2011) *A&A* 531:A106. [12] Mikouchi T. et al. (2023) 86th Annual Meeting of The Meteoritical Society, #6178. [13] Nakashima D. et al. (2012) *EPSL* 357-358:355. [14] Tenner T.J. et al. (2018) in *Chondrules: Records of Protoplanetary Disk Processes* 196. [15] Kurat G. et al. (1989) *Meteoritics* 24:35. [16] Jones R. H. et al. (2000) *M&PS* 35:849. [17] Ushikubo T. et al. (2012) *GCA* 90:242. [18] Yamanobe M. et al. (2018) *Polar Sci.* 15:29. [19] Chaumard N. et al. (2021) *GCA* 299:199. [20] Jacquet E. et al. (2021) *M&PS* 56:13. [21] Ushikubo T. & Kimura M. (2021) *GCA* 293:328. [22] Weisberg M. K. et al. (2021) *GCA* 300:279.

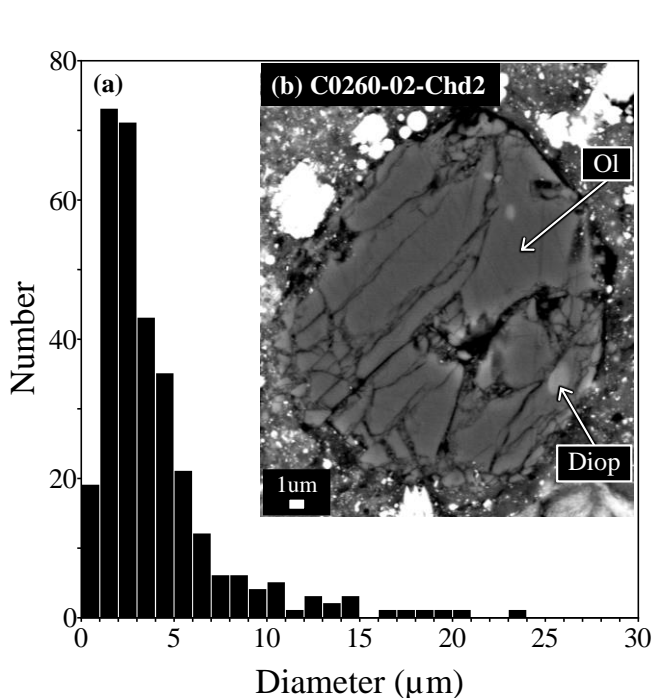


Fig. 1: Size distribution of anhydrous minerals including chondrule-like objects in C0224 and C0260 (a) and backscattered electron image of the chondrule-like object C0260-02-Chd2 (b). Ol, olivine; Diop, diopside.

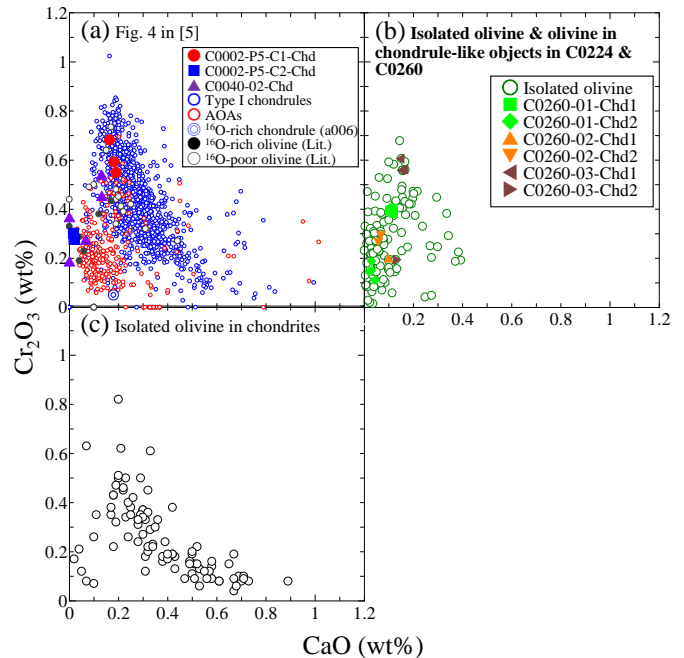


Fig. 2: Comparison of concentrations between Cr_2O_3 and CaO in olivine in chondrule-like objects, type I chondrules, AOAs, ^{16}O -rich and -poor chondrules (a), isolated olivine and olivine in chondrule-like objects in C0224 and C0260 (b), and isolated olivine in chondrites (c). The panel a is from Nakashima et al. [5]. Olivine data in the panel c are from [15-22].